# Economic Dispatch for Operating Cost Minimization under Real Time Pricing in Droop Controlled DC Microgrid

Li, Chendan; Federico, de Bosio; Chen, Fang; Chaudhary, Sanjay K.; Quintero, Juan Carlos Vasquez; Guerrero, Josep M.

*Published in:*
I E E E Journal of Emerging and Selected Topics in Power Electronics

*DOI (link to publication from Publisher):*
10.1109/JESTPE.2016.2634026

*Publication date:*
2017

*Document Version*
Early version, also known as pre-print



*Citation for published version (APA):*
Li, C., Federico, D. B., Chen, F., Chaudhary, S. K., Quintero, J. C. V., & Guerrero, J. M. (2017). Economic Dispatch for Operating Cost Minimization under Real Time Pricing in Droop Controlled DC Microgrid. *I E E E Journal of Emerging and Selected Topics in Power Electronics*, *5*(1), 587 - 595 . https://doi.org/10.1109/JESTPE.2016.2634026

# Economic Dispatch for Operating Cost Minimization under Real Time Pricing in Droop Controlled DC Microgrid

Chendan Li, *Student Member*, *IEEE*, Federico de Bosio, *Student Member*, *IEEE*, Fang Chen, *Student Member, IEEE,* Sanjay K. Chaudhary, *Member, IEEE,* Juan C. Vasquez, *Senior Member, IEEE and* Josep M. Guerrero, *Fellow*, *IEEE*

***Abstract*— In this paper, an economic dispatch problem for total operation cost minimization in DC microgrids is formulated. An operating cost is associated with each generator in the microgrid, including the utility grid, combining the cost-efficiency of the system with demand response requirements of the utility. The power flow model is included in the optimization problem, thus the transmission losses can be considered for generation dispatch. By considering the primary (local) control of the grid-forming converters of a microgrid, optimal parameters can be directly applied to this control level, thus achieving higher control accuracy and faster response. The optimization problem is solved in a heuristic method. In order to test the proposed algorithm, a six-bus droop-controlled DC microgrid is used in the case studies. Simulation results show that under variable renewable energy generation, load consumption and electricity prices, the proposed method can successfully reduce the operating cost by dispatching economically the resources in the microgrid.**

***Index Terms*— DC microgrids, demand response, economics, optimal power flow, genetic algorithm**

## NOMENCLATURE

| | |
|---|---|
| MGCC | Microgrid Centralized Controller |
| DG | Distributed Generation unit |
| ESS | Energy Storage System |
| $C_{utility}$ | Operating cost of the power from utility |
| $C_{ESS}$ | Operating cost of the storage system |
| $C_{FC}$ | Operating cost of the fuel cell |
| $C_{loss}$ | Cost of the transmission power losses |
| $C_{total}$ | Total operating cost of the microgrid |
| $\lambda_{buy}$ | Real-time utility electricity price |
| $\lambda_{sell}$ | Price of the electricity sold to the utility |
| $P_{utility}$ | Power exchanged with the utility |
| $P_{ESS}$ | Power exchanged by the storage system |
| $P_{renewable}$ | Power from renewable energy sources |
| $P_{Gi(DC)}$ | Generating power by the *i*-th unit |
| $P_{Di(DC)}$ | Consumed power by the *i*-th unit |
| $P_{loss}$ | Transmission power losses |
| $P_{Gi(DC)}$ | Power generated by the *i*-th unit |
| $P_{i(DC)}$ | Injection power by the *i*-th unit |
| $\Delta T$ | Number of optimization cycles in an hour |
| $\eta_{ch}$ | Efficiency during charging mode |
| $a_{ch}$, $b_{ch}$ | Linear coefficients of charge mode |
| $\eta_{dis}$ | Efficiency during discharging mode |
| $a_{dis}$, $b_{dis}$ | Linear coefficients of discharge mode |
| $a_{FC}$, $b_{FC}$, $c_{FC}$ | Coefficients of the fuel cell operating cost |
| $I_{Gi(DC)}$ | DC current to DC source |
| $I_{i(DC)}$ | DC injection current in bus *i* |
| $N_{g(DC)}$ | Number of dispatchable DG buses in DC microgrid |
| $N_{p(DC)}$ | Number of P buses in DC microgrid |
| $R_{vi(DC)}$ | Virtual resistance in DC microgrid |
| $R_{line\_ij}$ | Line resistance for line *ij* |
| $V_{i(DC)}$ | Voltage magnitude in bus *i* |
| $V_{Gi(DC)}$ | Output voltage to DC source |
| $V_{G0i(DC)}$ | Nominal output voltage to DC source |
| $Y_{ij(DC)}$ | Admittance between the bus *i* and bus *j* |

C. Li, S. K. Chaudhary, J. C. Vasquez and J. M. Guerrero are with the Department of Energy Technology, Aalborg University, 9220, Denmark. (e-mail: che@et.aau.dk; skc@et.aau.dk; juq@et.aau.dk; joz@et.aau.dk ).
Federico de Bosio is with the Department of Energy, Politecnico di Torino, 10124 Torino, Italy (e-mail: federico.debosio@polito.it)
Fang Chen is with the Center for Power Electronics Systems (CPES), Bradley Department of Electrical and Computer Engineering, Virginia Tech, Blacksburg, VA 24061 USA. (e-mail: fangchen@vt.edu)

## I. INTRODUCTION

NOWADAYS, with awakened increasing awareness of the environmental problems, Distributed Generators (DG) based on renewable energy sources are gaining more and more popularity. With anticipated high penetration of DGs, the traditional power system architecture consisting of large generation plants, transmission and distribution networks will be replaced by several microgrids in an intergrid scenario [1]-[3]. In this revolution, power electronic technology plays a fundamental role to match the different DGs output characteristics according to utility and customers' requirements. This issue becomes more salient when more and more modern loads, such as LEDs and power electronics devices, are installed in the building sector characterized by commercial

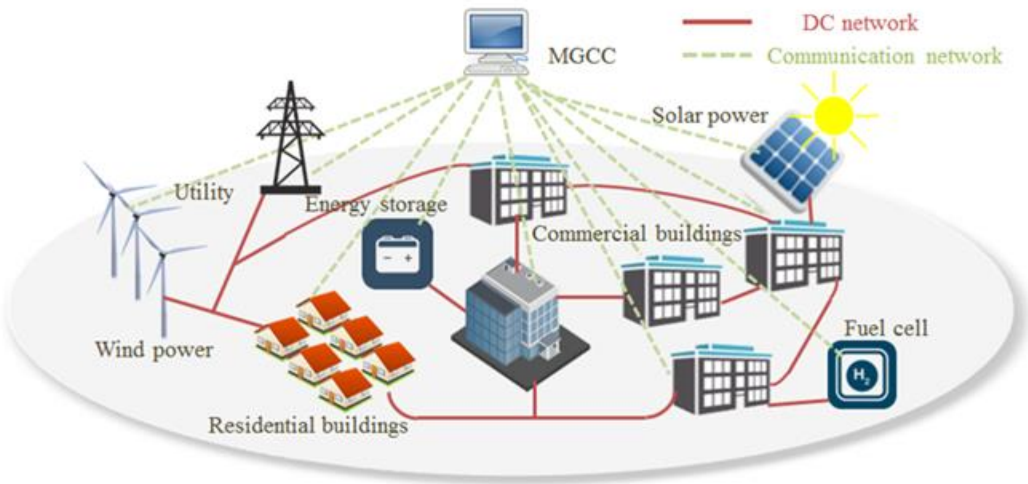


Fig. 1. Schematic of a DC microgrid operating at 380 V DC

TABLE I
INTERFACED RENEWABLE ENERGY SOURCES TYPOLOGIES

**Table 1 Interfaced renewable energy sources typologies**

| Conversion Classification | Converter Type |
|---|---|
| **DC bus to low voltage DC load** | DC-DC buck converter |
| **Wind power to DC bus** | AC-DC rectifier |
| **Fuel cell to DC bus** | DC-DC boost converter |
| **DC bus to/from ESS** | DC-DC buck-boost converter |
| **PV cell to DC bus** | DC-DC boost converter |

centres, data centres, residential communities and other similar facilities. To enhance system efficiency, considering the increasing energy demand to be supplied to more sophisticated appliances, DC distribution systems are proposed to interconnect DGs with modern loads, most of which are originally in DC. Previous research activities point out that using a common DC bus to supply different sources provides a simple structure with high efficiency, control and more reliable protections [4]-[6].

The DC microgrid, which will represent the fundamental element of the future intergrid, is expected to supply the loads at two DC voltage levels: a high-voltage bus and a low-voltage bus [7]-[10]. Low-voltage level operates at 48 V to meet the requirements of the majority of low voltage appliances, e.g. standard Telecom Communication (TLC) applications, portable computers, low power consumer electronics and light-emitting diode (LED) lighting. On the other hand, high power loads in commercial or residential buildings are supplied by a high-voltage bus operating between 360 V and 400 V DC, in order to reduce power losses. The rated voltage of 380 V DC is set to supply a huge amount of energy and comply with the voltage level in data centers [11]. This voltage level can be taken as the distribution voltage level in an intergrid based on DC microgrids. Fig. 1 shows a schematic of a DC grid operated at 380 V DC. The main components are represented by DGs based on renewable sources like solar and wind, battery Energy Storage Systems (ESS) and fuel cells. All these devices require a power converter to exchange energy within the microgrid. The necessary interfaced converters to connect different sources and loads are listed in Table I. Besides the electrical connections, a hierarchical communication control with low-speed data exchange is needed. By gathering the necessary information, like real-time electricity prices and load profiles, the energy manager can optimize the renewable energy utilization and increase system efficiency by means of economic dispatch.

## II. SYSTEM OPERATION COST COMPOSITION

A typical DC microgrid consists of a point of common coupling connected to the utility, and various DGs, such as battery ESS, fuel cells, wind power and PV systems. By neglecting the maintenance cost of these components, the correspondent operating costs can be identified as follows.

### *A. Utility Power Cost*

By considering the utility grid as a generation unit, its operating cost can be assessed according to the market price. With the development of "smart grid ready" technologies, including smart meters and technologies for bidirectional communications, customers can have access to real-time electricity prices and be involved more proactively with the power supplier in order to minimize the electricity cost [23]. Real-time pricing is one of the new forms of agreement between the customers and the supplier, which allows real-time demand response [24]. In this way, the operating cost of the power supplied by the utility in a corresponding control period ($C_{utility}$) can be modelled as:

$$C_{utility} = \begin{cases} \dfrac{\lambda_{buy} P_{utility}}{\Delta T}, & P_{utility} > 0 \\ \dfrac{\lambda_{sell} P_{utility}}{\Delta T}, & P_{utility} < 0 \end{cases} \tag{1}$$

where $\lambda_{buy}$ is the real-time utility electricity price, and $\lambda_{sell}$ is the price of electricity sold by the microgrid to the utility. Since the price here considered is hourly based, the optimization interval must be shorter than one hour, and thus the specific cost in one optimization interval is calculated by dividing for $\Delta T$, where $\Delta T$ is the number of optimization cycles in an hour.

### *B. Energy Storage Cost*

In this work, the operating cost of the ESS is modelled according to system efficiency. The major factors that influence its efficiency are the charging rate and the State of Charge (SOC), which can be modelled with the following linear relationship [16]:

$$\eta_{ch} = a_{ch} - b_{ch} P_{ESS} \tag{2}$$

where $\eta_{ch}$ is the charging efficiency, $a_{ch}$ and $b_{ch}$ are the linear coefficients of charging mode, and $P_{ESS}$ is the measured power flow from the DC microgrid to the ESS at its output terminals. This approximation considers only the charging rate, which is reasonable when dispatching is performed in a quasi-instantaneous way, since it has a large impact on the efficiency. On the other hand, during discharging mode, the efficiency in (2) can be rewritten as:

$$\eta_{dis} = a_{dis} + b_{dis} P_{ESS} \tag{3}$$

where $\eta_{dis}$ is the discharging efficiency, $a_{dis}$ and $b_{dis}$ are the linear coefficients of discharging mode. The operating cost can now be calculated depending on the charging (PESS>0) or discharging (PESS<0) mode as follows:

$$C_{ESS} = \begin{cases} \dfrac{\lambda_{buy}(\mathrm{P}_{ESS} - \eta_{ch}\,\mathrm{P}_{ESS})}{\Delta T}, & P_{ESS} > 0 \\ \dfrac{\lambda_{sell}(P_{ESS} - P_{ESS}/\eta_{dis})}{\Delta T}, & P_{ESS} < 0 \end{cases} \tag{4}$$

where $C_{ESS}$ is the operating cost of the ESS.

### C. *Fuel cell costs*

The fuel consumed by the fuel cell generators can be modelled according to a quadratic relationship of the output power [25]. Hence, the operating cost of this device can be modelled as follows:

$$C_{FC} = \frac{a_{FC} P_{FC}^2 + b_{FC} P_{FC} + c_{FC}}{\Delta T} \tag{5}$$

where $a_{FC}$, $b_{FC}$, $c_{FC}$ are all constant coefficients.

### D. *Renewable Energy Cost*

The fuel cost of renewable energy is free. To maximize the renewable energy generation, the operating cost of them in this study is set to zero, due to its negligible value compared to the fuel cost associated to traditional generators. Notice here that the cost occurred by maintenance is not considered in the optimization.

### E. *Transmission Power Losses Cost*

The transmission power losses do not belong to any generation unit. In fact, they are the result of how power is dispatched, which is actually incorporated explicitly in the utility cost, since an accurate power flow model is added as a constraint. To underline this issue, the following equation can be added to the system cost model:

$$C_{loss} = \frac{\lambda_{buy} P_{loss}}{\Delta T} \tag{6}$$

being $P_{loss}$ the transmission power losses. The exact transmission power losses can be calculated by running the power flow algorithm, which is further explained in the next section.

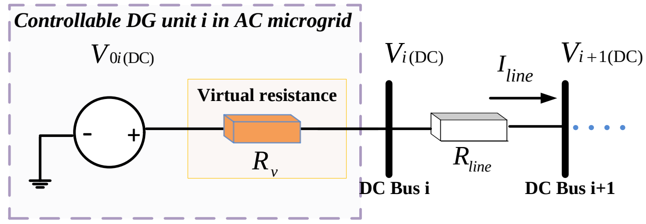


Fig. 2 Virtual resistance control concept in DC microgrids

## III. Power Flow for DC Microgrid

Power flow is an important tool not only for optimal planning but also to assure optimal operation [26]. In DC microgrid power flow modelling, two types of buses can be defined. All the loads and non-dispatchable DG units can be labelled as P buses. On the other hand, dispatchable DG units can be represented by dispatchable DG buses, which are assumed to work in droop control mode during normal operation.

Compared to AC microgrids, this droop control algorithm is not directly based on the generated power, but it is realized by feeding back the output current through a virtual resistance [1], [27], [28]. In AC microgrids, the virtual impedance is adopted to change the output impedance of the converter to cancel out the effect of active and reactive power coupling, as well as providing proper current sharing between power converters modules in case of line unbalance. On the other hand, in DC microgrids, virtual impedance is employed directly for power sharing, which is responsible for droop control.

In case of dispatchable DG buses, the concept of droop control using virtual resistance can be simplified as shown in Fig. 2. This regulation is expressed by [29], [30]:

$$V_{i(\mathrm{DC})} = V_{Gi(\mathrm{DC})} = V_{0i(\mathrm{DC})} - R_{vi(\mathrm{DC})} I_{Gi(\mathrm{DC})} \tag{7}$$

where $V_{Gi(\mathrm{DC})}$ is the output voltage of a DC source, which is also the bus voltage in bus *i*, $V_{0i(\mathrm{DC})}$ is the nominal voltage, $I_{Gi(\mathrm{DC})}$ is the output current, and $R_{vi(\mathrm{DC})}$ is the virtual resistance in the dispatchable DG unit *i*. $I_{Gi(\mathrm{DC})}$ can be written as:

$$I_{Gi(\mathrm{DC})} = \frac{P_{Gi(\mathrm{DC})}}{V_{i(\mathrm{DC})}} \tag{8}$$

where $P_{Gi(\mathrm{DC})}$ is the power generated by unit *i*.

The network of DC microgrids can be considered as pure resistive in the steady-state model. According to Kirchhoff's current law, the network equation for both types of buses can thus be written as follows:

$$I_{i(\mathrm{DC})} = \sum_{\substack{j=1 \\ j\neq i}}^{n} Y_{ij(\mathrm{DC})}(V_{i(\mathrm{DC})} - V_{j(\mathrm{DC})}) \tag{9}$$

where $I_{i(\mathrm{DC})}$ is the DC injection current in bus *i*, $Y_{ij(\mathrm{DC})}$ is the admittance between bus *i* and bus *j*, and $V_{i(\mathrm{DC})}$ is the voltage magnitude in bus *i*. In a unipolar DC microgrid, the injection power has the following relationship with the injection current:

$$P_{i(\mathrm{DC})} = V_{i(\mathrm{DC})} I_{i(\mathrm{DC})} \tag{10}$$

Thus, (10) can also be written as:

$$P_{i(\mathrm{DC})} = V_{i(\mathrm{DC})} \sum_{\substack{j=1 \\ j \neq i}}^{n} Y_{ij(\mathrm{DC})} (\mathrm{V}_{i(\mathrm{DC})} - V_{j(\mathrm{DC})}) \tag{11}$$

For similarity, the non-dispatchable DG units can be interpreted as negative loads. Considering the real power balance of the system, the whole mathematical model can be formulated as follows:

$$V_{0i(\mathrm{DC})} - R_{vi(\mathrm{DC})} \frac{P_{Gi(\mathrm{DC})}}{V_{i(\mathrm{DC})}} - V_{i(\mathrm{DC})} = 0 \tag{12}$$

$$P_{Gi(\mathrm{DC})} - P_{Di(\mathrm{DC})} - P_{i(\mathrm{DC})} = 0 \tag{13}$$

The number of total mismatch functions is $N_{(\mathrm{DC})}$ ,as expressed in:

$$N_{(\mathrm{DC})} = 2 \times N_{g(\mathrm{DC})} + N_{p(\mathrm{DC})} \tag{14}$$

where $N_{g(\mathrm{DC})}$ is the number of dispatchable DG buses, and $N_{p(\mathrm{DC})}$ is the number of P buses. The number of unknown variables should be equal to the number of mismatch functions in the model; in this way the power flow has a unique solution. The unknown variables include the voltage at each bus and the power generated from each dispatchable DG unit. Therefore, the system can be solved by trust-region dogleg algorithms, like for AC microgrids [22][31].

How different control parameters affect the whole system can be obtained by solving the equations of the power flow model. Finally, power transmission losses can be calculated by running the power flow.

## IV. System Operation Cost Composition

### *A. Objective function*

The objective of this study is to minimize the total operating cost in one optimization cycle in the context of real-time pricing. Accordingly, renewable energy resources, ESS and backup generation systems are coordinated in a highly efficient way, while still achieving demand response. Considering a microgrid in which each type of generation system has only one unit, the total cost can be calculated through (1) − (6) as:

$$C_{total} = C_{utility} + C_{ESS} + C_{FC} + C_{loss} \tag{15}$$

In this way the economic benefits of the microgrid owner can be maximized. This objective can be written as:

$$\overset{Minimize}{C_{total}} (\mathrm{x}_i) \tag{16}$$

where $\mathrm{x}_i$ indicates the optimization variables which are also the control variables of dispatchable units. Although nominal voltage $V_{0i(\mathrm{DC})}$ can also be controlled to achieve power regulation. Here the virtual impedance $R_{vi(\mathrm{DC})}$ of the grid forming unit is taken as the optimization variable, leading to the following problem formulation:

$$\overset{Minimize}{C_{total}} (\mathrm{u}, R_{vi}) \tag{17}$$

where *u* are, in general, the unknown state variables of the system, which can be calculated in the power flow analysis discussed in last section.

### *B. Constraints*

The constraints of the optimization problem include the system constraints and those from each generation system. The first system constraint is the overall power flow balance, which can be written as:

$$P_{renewable} + P_{utility} + P_{FC} - P_{ESS} - P_{load} - P_{loss} = 0 \tag{18}$$

This equation is satisfied by the convergence of the power flow algorithm using the method provided in [22]. The second system constraint considers the life cycle of the ESS. This component is not allowed to operate in discharging mode while energy is flowing from microgrid into the utility grid. The main reason is because it reduces the ESS efficiency if the energy flows through the batteries twice. Moreover, according to present normative in different countries, it is not allowed to discharge energy from batteries into the grid.

Additional constraints including droop control equation (12) and power balance equation (13), with the boundaries for $R_{vi}$ and the DC voltage at each node $V_{i(\mathrm{DC})}$ are:

$$0 < R_{vi} < R_{vi,\max} \tag{19}$$

$$\mathrm{V}_{i(\mathrm{DC}),\min} < \mathrm{V}_{i(\mathrm{DC})} < \mathrm{V}_{i(\mathrm{DC}),\max} \tag{20}$$

For each dispatchable unit, the power delivered should be maintained within their respective capacity limits, which can be expressed as:

$$P_{utility,\min} < P_{utility} < P_{utility,\max} \tag{21}$$

$$P_{ESS,\min} < P_{ESS} < P_{ESS,\max} \tag{22}$$

$$0 < P_{FC} < P_{FC,\max} \tag{23}$$

All the inequality constraints are included in the model by adding a large value to the objective function as penalty whenever a bound is violated.

### *C. Heuristic optimization based on GA*

Genetic Algorithm is chosen for optimization in this work. Compared to other similar optimization algorithms, some main advantages of GA can be identified [32][33]: i) the computation of the derivative of the objective function is not required, i.e. the opposite compared to optimization algorithms based on gradient method; ii) the risk to be trapped in local optimum is reduced; iii) a large number of variables can be processed while still providing a list of optimum solutions.

The basic idea of the algorithm is that better individuals of a population get higher chances to survive, which probability is proportional to a fitness function, strictly related to the objective function of the problem. Two main search operators known as crossover and mutation allow the algorithm to privilege exploration and exploitation, respectively. Crossover selects randomly a point on two binary strings (parents), splitting them at this crossover point. Children are then created by exchanging tails. On the other hand, mutation alters gene

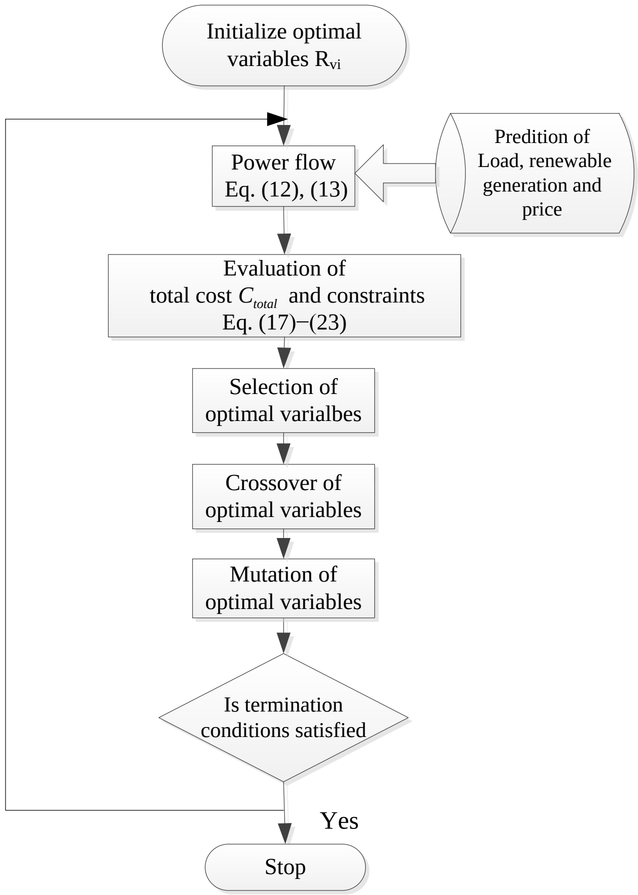


Fig. 3. Flow chart of the problem

independently according to a pre-defined probability. In Fig.3 a flow chart representation of the main steps involved in the optimization algorithm is reported.

## V. Case Study

### A. Input Data

The proposed methodology is applied to minimize the operating cost of a 380 V six-bus DC microgrid as shown in Fig. 4. The test case consists of one P bus with renewable energy sources based on wind turbines and PV panels (Bus 1), three dispatchable DG buses interfaced with ESS (Bus 2), utility (Bus 3) and fuel cell (Bus 6), and two other P buses feeding the load (Bus 4 and 5). In this work the distributed generators and its interfaced converter are considered as a single component. Instead of using a traditional radial topology, the network adopts a meshed configuration to increase system reliability. Network data are given as listed in Table II. The capacity constraints of the DGs are reported in Table III.

To test the effectiveness of the algorithm in the context of time changing price, simulation tests are repeatedly conducted in a 24-hour span. The real-time data are taken from the website of the regional transmission organization PMJ [34], and the renewable generation data are obtained from Open Energy Information (OpenEI) [35]. The generation profiles of the wind turbines and solar panels at bus 2 and the load profiles at bus 4

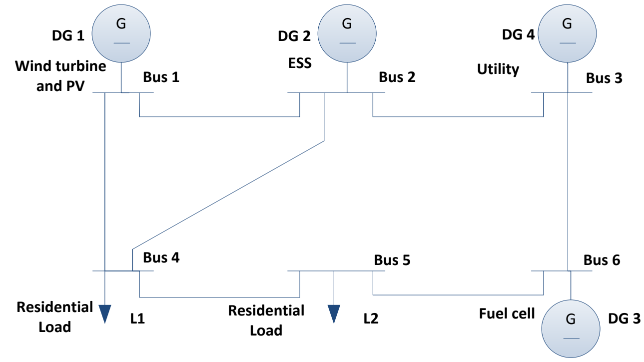


Fig. 4 Single line diagram of an example DC microgrid

TABLE II
Lines Impedance of the Network

| Line No. | From Bus | To Bus | R (pu) | Length (m) |
|---|---|---|---|---|
| **1** | 1 | 2 | 0.0058 | 200 |
| **2** | 1 | 4 | 0.0087 | 300 |
| **3** | 2 | 4 | 0.004 | 140 |
| **4** | 4 | 5 | 0.0058 | 200 |
| **5** | 5 | 6 | 0.0029 | 100 |
| **6** | 3 | 6 | 0.0043 | 150 |
| **7** | 2 | 3 | 0.0049 | 170 |

TABLE III
Capacity Limits of Each Generation Unit

| Generation Unit | Utility | Energy Storage | Fuel Cell |
|---|---|---|---|
| Capacity limits (KW) | (-30,30) | (-30,30) | (0,30) |

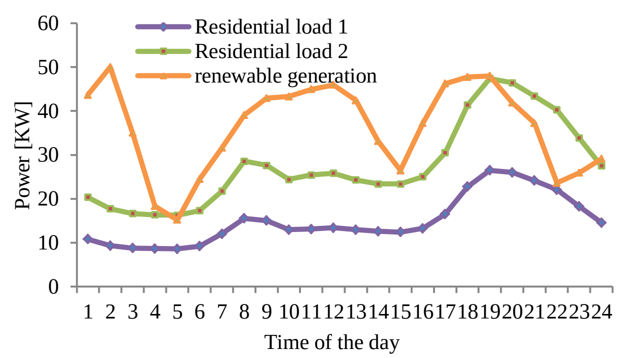


Fig. 5. Load and renewable generation profile

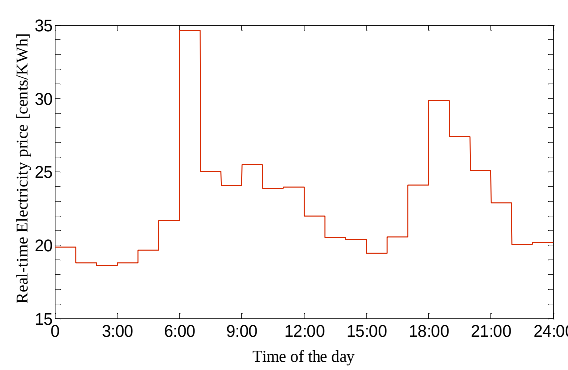


Fig. 6. Real-time price profile

TABLE IV
Genetic Algorithm Parameters

| Parameter | |
|---|---|
| **Number of population** | 12 |
| **Max number of generation** | 25 |
| **Mutation rate** | 0.2 |
| **Selection rate** | 0.5 |
| **Initialized R1/R2/R3** | 0.01/0.3/0.3Ω |

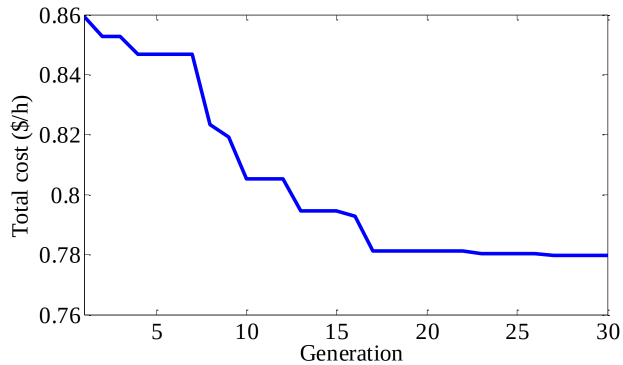


Fig. 7. Convergence trace of the optimization algorithm for the 22th hour

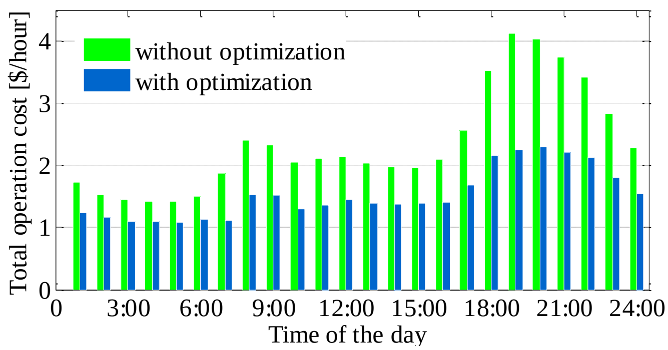


Fig. 8. Total operation cost comparison.

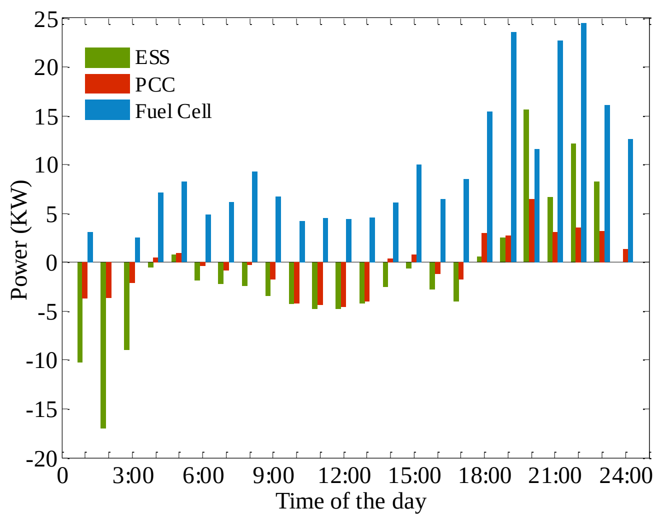


Fig. 9 Optimal generation dispatch results

and 5 are shown in Appendix, and in Fig. 5 and Fig. 6. Parameters related to GA for optimization are listed in Table 4. These parameters are chosen as a trade-off between optimization accuracy and computational time effort.

### *B. Results and discussion*

Firstly, to test the performance of GA algorithm, optimization for a single hour is conducted based on the input data from the 22th hour. Fig. 7 shows the convergence trace of the proposed GA for optimal power flow algorithm. It can be seen that, after 25 generations, the total cost starts to converge.

The daily total operating cost using optimization is compared with the one without optimization, as shown in Fig. 8, in which the virtual impedance for utility, fuel cell, and energy storage is initially set at 0.1 Ω, 0.3 Ω and 0.3 Ω respectively. The

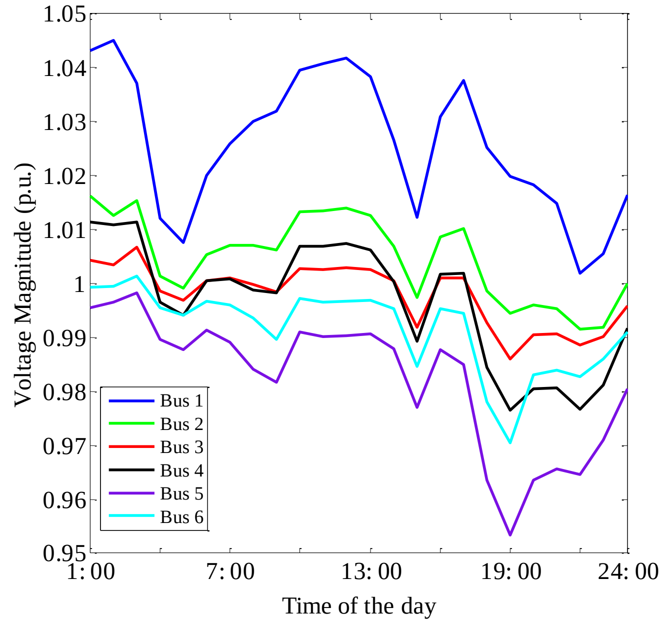


Fig. 10. Voltage profile of optimization results

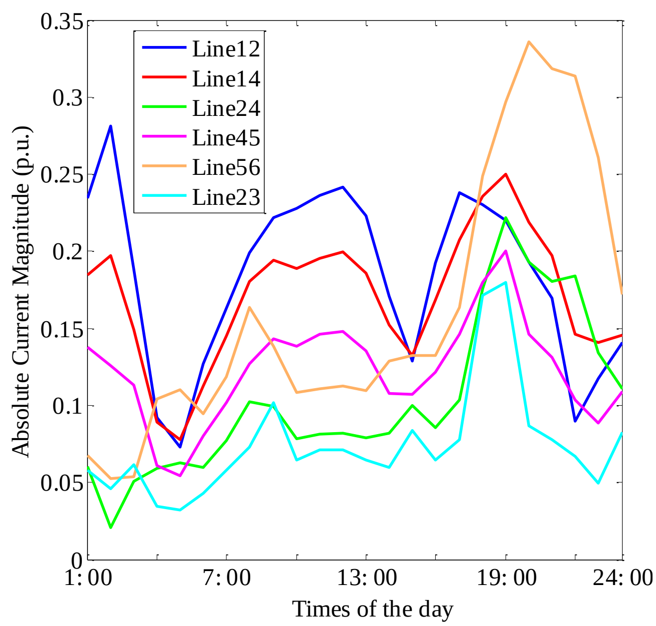


Fig. 11. Current profile of optimization results

comparison shows that by dispatching optimally the resources, the total operating cost is considerably reduced. The dispatch results of each hour in a day are shown in Fig. 9, where no violation of the power constraints is observed. Fig. 10 and Fig 11 illustrate the voltage profile of each bus and current magnitude of each transmission line in these 24 scenarios, respectively. It can be seen that the voltage vacillation is within the allowable range and the current shows no violation either.

## VI. CONCLUSIONS

In order to improve the system efficiency of a 380 V DC microgrid network while participating in demand response, an optimal power flow problem is formulated. The cost function represents not only the operating cost within the microgrid incurred by the fuel and efficiency of the components and the power flows in the transmission line, but also the demand response requirements from the utility by considering real-time pricing. The proposed algorithm is implemented by means of a heuristic method based on GA. A six-bus DC microgrid is tested to verify the proposed algorithm in a 24-hour span. Test results show that GA can find the optimal control parameters to optimally manage the dispatchable resources. Finally, the proposed algorithm successfully reduces the operating cost compared to the case study in which the system is managed without optimization.

## APPENDIX

Table 5 shows the renewable generation, load profile, and real-time price profile [34][35]. The residential load data is calibrated according to the real data from OpenEI, and the renewable generation data is combining both the solar and wind generation according to the data got also from OpenEI, and the price data are referred to the real data from PJM Market Price Information

TABLE V
RENEWABLE GENERATION, LOAD AND REAL PRICE PROFILES

| hour | L1 [KW] | L2 [KW] | DGs [KW] | Price [cents/KWh] |
|---|---|---|---|---|
| **1:00** | 10.84 | 20.39 | 43.66 | 19.86 |
| **2:00** | 9.35 | 17.74 | 50.00 | 18.79 |
| **3:00** | 8.78 | 16.67 | 35.02 | 18.64 |
| **4:00** | 8.67 | 16.36 | 18.35 | 18.79 |
| **5:00** | 8.61 | 16.26 | 15.21 | 19.68 |
| **6:00** | 9.24 | 17.30 | 24.47 | 21.67 |
| **7:00** | 12.03 | 21.76 | 31.59 | 34.62 |
| **8:00** | 15.58 | 28.59 | 39.08 | 25.05 |
| **9:00** | 15.07 | 27.64 | 42.95 | 24.06 |
| **10:00** | 13.00 | 24.41 | 43.31 | 25.47 |
| **11:00** | 13.14 | 25.43 | 44.93 | 23.85 |
| **12:00** | 13.41 | 25.83 | 45.96 | 23.97 |
| **13:00** | 12.98 | 24.30 | 42.41 | 21.97 |
| **14:00** | 12.60 | 23.39 | 33.15 | 20.54 |
| **15:00** | 12.44 | 23.40 | 26.48 | 20.37 |
| **16:00** | 13.28 | 25.05 | 37.20 | 19.44 |
| **17:00** | 16.50 | 30.51 | 46.24 | 20.56 |
| **18:00** | 22.77 | 41.35 | 47.76 | 24.11 |
| **19:00** | 26.50 | 47.42 | 47.98 | 29.84 |
| **20:00** | 26.02 | 46.42 | 41.92 | 27.39 |
| **21:00** | 24.17 | 43.41 | 37.26 | 25.11 |
| **22:00** | 22.11 | 40.27 | 23.63 | 22.88 |
| **23:00** | 18.31 | 33.90 | 25.93 | 20.04 |
| **24:00** | 14.60 | 27.52 | 29.12 | 20.18 |

## REFERENCES


[1] J. M. Guerrero, J. C. Vasquez, J. Matas, L. G. de Vicuna, and M. Castilla, "Hierarchical Control of Droop-Controlled AC and DC MicrogridsA General Approach Toward Standardization," *IEEE Trans. Ind. Electron.*, vol. 58, pp. 158–172, 2011.

[2] D. Boroyevich, I. Cvetković, D. Dong, R. Burgos, F. Wang, and F. Lee, "Future electronic power distribution systems - A contemplative view," *Proc. Int. Conf. Optim. Electr. Electron. Equipment*, OPTIM, pp. 1369–1380, 2010.

[3] D. Boroyevich, I. Cvetkovic, R. Burgos, and D. Dong, "Intergrid: A Future Electronic Energy Network?," *IEEE J. Emerg. Sel. Top. Power Electron.*, vol. 1, pp. 127–138, 2013.

[4] M. Rodriguez, G. Stahl, L. Corradini, and D. Maksimovic, "Smart DC Power Management System Based on Software-Configurable Power Modules," *IEEE Trans. Power Electron*., vol. 28. pp. 1571–1586, 2013.

[5] F. Chen, R. Burgos, D. Boroyevich, and D. Dong, "Control loop design of a two-stage bidirectional AC/DC converter for renewable energy systems," *in 2014 IEEE Applied Power Electronics Conference and Exposition-APEC 2014*, 2014, pp. 2177–2183.

[6] K. Strunz, E. Abbasi, and D. N. Huu, "DC Microgrid for Wind and Solar Power Integration," *Emerg. Sel. Top. Power Electron. IEEE J.*, vol. 2, pp. 115–126, 2014.

[7] P, S. Karlsson, and J., "DC Bus Voltage Control for a Distributed Power System," *IEEE Trans. Power Electron*., vol. 18, pp. 1405–1412, 2003.

[8] F. Chen; R. Burgos; D. Boroyevich; X. Zhang, "Low-Frequency Common-Mode Voltage Control for Systems Interconnected with Power Converters," *IEEE Trans. Ind. Electron.*, vol.PP, no.99, pp.1-1

[9] D. Nilsson and A. Sannino, "Efficiency analysis of low- and medium-voltage DC distribution systems," in *Power Engineering Society General Meeting*, 2004. IEEE, 2004, pp. 2315-2321 Vol.2.

[10] I. Cvetkovic, D. Boroyevich, and F. Lee, "Future home DC-based renewable energy nanoGrid system," *Conf. Gd. Challenges Model. Simul.*, 2010.

[11] F. Bodi, and E. H. Lim, "Criteria for emerging telecom and data center powering architectures," in *INTELEC, International Telecommunications Energy Conference (Proceedings)*, 2012.

[12] F. Chen, W. Zhang, R. Burgos, and D. Boroyevich, "Droop voltage range design in DC micro-grids considering cable resistance," in *2014 IEEE Energy Conversion Congress and Exposition, ECCE 2014*, 2014, pp. 770–777.

[13] Yunjie Gu, Wuhua Li, Xiangning He, "Frequency-Coordinating Virtual Impedance for Autonomous Power Management of DC Microgrid", *IEEE Trans. Power Electron.*, vol. 30, pp. 2328-2337, 2015, ISSN 0885-8993..

[14] X. Lu, J. M. Guerrero, K. Sun, and J. C. Vasquez, "An Improved Droop Control Method for DC Microgrids Based on Low Bandwidth Communication With DC Bus Voltage Restoration and Enhanced Current Sharing Accuracy," *IEEE Trans. Power Electron*., vol.29, no.4, pp.1800-1812, April 2014

[15] L. Meng, T. Dragicevic, J. Roldán-Pérez, J. C. Vasquez and J. M. Guerrero, "Modeling and Sensitivity Study of Consensus Algorithm-Based Distributed Hierarchical Control for DC Microgrids," *IEEE Trans. Smart Grid*, vol. 7, no. 3, pp. 1504-1515, May 2016

[16] Y. Xu, W. Zhang, G. Hug, S. Kar, and Z. Li, "Cooperative control of distributed energy storage systems in a microgrid," *IEEE Trans. Smart Grid*, vol. 6, pp. 238–248, 2015.

[17] H. Mohsenian-Rad, and A. Davoudi, "Towards Building an Optimal Demand Response Framework for DC Distribution Networks," *IEEE Trans. Smart Grid*, vol.5, no.5, pp.2626 - 2634, Sept. 2014

[18] L. Che, and M. Shahidehpour, "DC Microgrids: Economic Operation and Enhancement of Resilience by Hierarchical Control," *IEEE Trans. Smart Grid*, vol.5, no.5, pp.2517 - 2526, Sept. 2014

[19] F. A. Mohamed, and H. N. Koivo, "Online Management of MicroGrid with Battery Storage Using Multiobjective Optimization," *Power Engineering, Energy and Electrical Drives, 2007. POWERENG 2007. International Conference on*, vol., no., pp.231,236, 12-14 April 2007

[20] O. Erdinc, N. G. Paterakis, T. D. P. Mendes, A. G. Bakirtzis and J. P. S. Catalão, "Smart Household Operation Considering Bi-Directional EV and ESS Utilization by Real-Time Pricing-Based DR," *IEEE Trans. Smart Grid*, vol. 6, no. 3, pp. 1281-1291, May 2015. DOI: 10.1109/TSG.2014.2352650

[21] C. Li; S. K. Chaudhary; M. Savaghebi; J. C. Vasquez; J. M. Guerrero, "Power Flow Analysis for Low-voltage AC and DC Microgrids Considering Droop Control and Virtual Impedance," *IEEE Trans. Smart Grid*, vol.PP, no.99, pp.1-1

[22] Smart Grid Strategy. The intelligent energy system of the future. Danish Ministry of Climate, Energy and Building, May 2013. [Online]. Available: http://www.ienergi.dk/~/media/BFIE/Filer/Regeringens_Smart_Grid_Strategy_UK_web.ashx

[23] A. J. Conejo, J. M. Morales, and L. Baringo, "Real-Time Demand Response Model," *IEEE Trans. Smart Grid*, vol.1, no.3, pp.236,242, Dec. 2010

[24] M. Y. Nguyen and Y. T. Yoon, “A Comparison of Microgrid Topologies Considering Both Market Operations and Reliability,” *Electr. Power Components Syst.*, vol. 42, pp. 585–594, 2014.

[25] T. Ersal, C. Ahn, D. L. Peters, J. W. Whitefoot, A. R. Mechtenberg, I. A. Hiskens, H. Peng, A. G. Stefanopoulou, P. Y. Papalambros, and J. L. Stein, “Coupling between component sizing and regulation capability in microgrids,” *IEEE Trans. Smart Grid*, vol. 4, pp. 1576–1585, 2013.

[26] D. Chen, and L. Xu, "Autonomous DC Voltage Control of a DC Microgrid With Multiple Slack Terminals," *IEEE Trans. Power Syst.*, vol.27, no.4, pp.1897,1905, Nov. 2012

[27] P. Karlsson, and J. Svensson, "DC bus voltage control for a distributed power system," *IEEE Trans. Power Electron.*, vol.18, no.6, pp.1405,1412, Nov. 2003

[28] C. Li, S. K. Chaudhary, T. Dragicevic, J. C. Vasquez, and J. M. Guerrero, “Power flow analysis for DC voltage droop controlled DC microgrids,” *in 11th International Multi-Conference on Systems*, Signals Devices (SSD), 2014, pp. 1–5.

[29] C. Li, S. K. Chaudhary, J. C. Vasquez, and J. M. Guerrero, “Power flow analysis for droop controlled LV hybrid AC-DC microgrids with virtual impedance,” in *2014 IEEE PES General Meeting | Conference & Exposition*, 2014, pp. 1–4.

[30] J. Nocedal and S. J. Wright, Trust-Region Methods, *Numerical Optimization, 2nd ed*. New York: Springer, 1999, ch. 4, pp. 66–100.

[31] R. L. Haupt and S. E. Haupt, Practical Genetic Algorithms, 2nd ed. Hoboken, NJ, USA: Wiley, Apr. 21, 2014. [Online]. Available:http://onlinelibrary.wiley.com/book/10.1002/0471671746;jsessionid=68B5F5913141E057EEE8CC9161628F2F.f01t3

[32] A. G. Bakirtzis, P. N. Biskas, C. E. Zoumas, and V. Petridis, "Optimal Power Flow by Enhanced Genetic Algorithm," *Power Engineering Review*, IEEE, vol.22, no.2, pp.60,60, Feb. 2002

[33] Website of the regional transmission organization PMJ. http://www.pjm.com

[34] Open Energy Information (OpenEI), website: http://en.openei.org


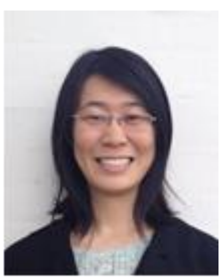

**Chendan Li** (S’13) received the B.S. degree and M.S. degree in Electrical Engineering from Nanjing Agricultural University, Nanjing Univ. of Aeronautics & Astronautics, Nanjing, Jiangsu, China, in 2009 and 2012 respectively.

She is currently working toward the Ph.D. degree in the Department of Energy Technology at Aalborg University, Aalborg, Denmark, as a member in the Microgrids Research Programme. Her main research interests include steady state and dynamic analysis, optimization and distributed control for AC and DC microgrid.

**Federico de Bosio** (S’14) was born in Torino, Italy, in 1989. He received the B.S. and M.Sc. degrees from the Politecnico di Torino, Turin, Italy, in 2011 and 2013, respectively.

Since 2014 he is pursuing the Ph.D. degree in Electrical, Electronics and Telecommunications Engineering at the Politecnico di Torino.

In 2015 he was a Ph.D. guest at the Department of Energy Technology of Aalborg University, working on control of power converters for islanded microgrids/UPS systems. His main research interests include control of power converters, energy storage systems and optimal energy management.

**Sanjay K. Chaudhary** (S’01–M’11) obtained his M. Tech. (Electrical Engg.) in 2002 from Indian Institute of Technology, Kanpur, India. He received his Ph.D. from Aalborg University, Denmark in 2011.

He worked with ABB Ltd. India from 2002 to 2005 and with Honeywell Technology Solutions Lab, Bangalore from 2005-2008. In July 2011, he joined the Department of Energy Technology, Aalborg University as Assistant Professor. Since July 2015, he is employed as Associate Professor.

His main interest is on grid integration of renewable energy, application of power converters in power system, HVDC and FACTS.

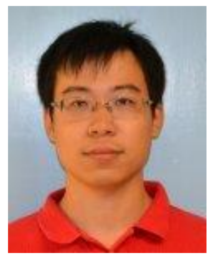

**Fang Chen** (S’13) received the Bachelor’s and Master’s degrees from Zhejiang University, Hangzhou, China in 2009 and 2012 respectively.He is now pursuing his Ph.D. degree in the Center for Power Electronics Systems (CPES) at Virginia Polytechnic Institute and State University (Virginia Tech), Blacksburg, VA, USA. From 2015 to 2016, he was a guest student at the Department of Energy Technology, Aalborg University, Aalborg, Denmark.

His research interests include operation and control of dc power distribution systems, net-zero-energy buildings, and design of ac-dc converters for utility applications.

**Juan C. Vasquez** (M’12-SM’14) received the B.S. degree in electronics engineering from the Autonomous University of Manizales, Manizales, Colombia, and the Ph.D. degree in automatic control, robotics, and computer vision from the Technical University of Catalonia, Barcelona, Spain, in 2004 and 2009, respectively. He was with the Autonomous University of Manizales working as a teaching assistant and the Technical University of Catalonia as a Post-Doctoral Assistant in 2005 and 2008 respectively. In 2011, he was Assistant Professor and from 2014 he is working as an Associate Professor at the Department of Energy Technology, Aalborg University, Denmark where he is the Vice Programme Leader of the Microgrids Research Program. From Feb. 2015 to April. 2015 he was a Visiting Scholar at the Center of Power Electronics Systems (CPES) at Virginia Tech. His current research interests include operation, advanced hierarchical and cooperative control, optimization and energy management applied to distributed generation in AC and DC microgrids. He has authored and co-authored more than 100 technical papers only in Microgrids where 60 of them are published in international IEEE journals.

Dr. Vasquez is currently a member of the IEC System Evaluation Group SEG4 on LVDC Distribution and Safety for use in Developed and Developing Economies, the Renewable

Energy Systems Technical Committee TC-RES in IEEE Industrial Electronics, PELS, IAS, and PES Societies.

**Josep M. Guerrero** (S'01-M'04-SM'08-FM'15) received the B.S. degree in telecommunications engineering, the M.S. degree in electronics engineering, and the Ph.D. degree in power electronics from the Technical University of Catalonia, Barcelona, in 1997, 2000 and 2003, respectively. Since 2011, he has been a Full Professor with the Department of Energy Technology, Aalborg University, Denmark, where he is responsible for the Microgrid Research Program. From 2012 he is a guest Professor at the Chinese Academy of Science and the Nanjing University of Aeronautics and Astronautics; from 2014 he is chair Professor in Shandong University; and from 2015 he is a distinguished guest Professor in Hunan University.

His research interests is oriented to different microgrid aspects, including power electronics, distributed energy-storage systems, hierarchical and cooperative control, energy management systems, and optimization of microgrids and islanded minigrids; recently specially focused on maritime microgrids for electrical ships, vessels, ferries and seaports. Prof. Guerrero is an Associate Editor for the IEEE TRANSACTIONS ON POWER ELECTRONICS, the IEEE TRANSACTIONS ON INDUSTRIAL ELECTRONICS, and the IEEE Industrial Electronics Magazine, and an Editor for the IEEE TRANSACTIONS on SMART GRID and IEEE TRANSACTIONS on ENERGY CONVERSION. He has been Guest Editor of the IEEE TRANSACTIONS ON POWER ELECTRONICS Special Issues: Power Electronics for Wind Energy Conversion and Power Electronics for Microgrids; the IEEE TRANSACTIONS ON INDUSTRIAL ELECTRONICS Special Sections: Uninterruptible Power Supplies systems, Renewable Energy Systems, Distributed Generation and Microgrids, and Industrial Applications and Implementation Issues of the Kalman Filter; and the IEEE TRANSACTIONS on SMART GRID Special Issue on Smart DC Distribution Systems. He was the chair of the Renewable Energy Systems Technical Committee of the IEEE Industrial Electronics Society. He received the best paper award of the IEEE Transactions on Energy Conversion for the period 2014-2015. In 2014 and 2015 he was awarded by Thomson Reuters as Highly Cited Researcher, and in 2015 he was elevated as IEEE Fellow for his contributions on "distributed power systems and microgrids."